Journal of Computational Physics **148,** 341–365 (1999)
Article ID jcph.1998.6114, available online at http://www.idealibrary.com on IDEAL®

# A Stable and Conservative Interface Treatment of Arbitrary Spatial Accuracy

Mark H. Carpenter,* Jan Nordström,† and David Gottlieb‡,[1]

*Aerodynamic and Acoustic Methods Branch, NASA Langley Research Center, Hampton, Virginia 23681-2199; †Computational Aerodynamics Department, FFA, The Aeronautical Research Institute of Sweden, Bromma, Sweden; ‡Division of Applied Mathematics, Brown University, Providence, Rhode Island 02912
E-mail: m.h.carpenter@larc.nasa.gov, nmj@ffa.se, dig@cfm.brown.edu

Received February 10, 1998; revised September 9, 1998

Stable and accurate interface conditions based on the SAT penalty method are derived for the linear advection–diffusion equation. The conditions are functionally independent of the spatial order of accuracy and rely only on the form of the discrete operator. We focus on high-order finite-difference operators that satisfy the summation-by-parts (SBP) property.We prove that stability is a natural consequence of the SBP operators used in conjunction with the new, penalty type, boundary conditions. In addition, we show that the interface treatments are conservative. The issue of the order of accuracy of the interface boundary conditions is clarified. New finite-difference operators of spatial accuracy up to sixth order are constructed which satisfy the SBP property. These finite-difference operators are shown to admit design accuracy ($p$th-order global accuracy) when $(p-1)$th-order stencil closures are used near the boundaries, if the physical boundary conditions and interface conditions are implemented to at least $p$th-order accuracy. Stability and accuracy are demonstrated on the nonlinear Burgers' equation for a 12-subdomain problem with randomly distributed interfaces. 

*Key Words:* high-order finite-difference; numerical stability; interface conditions; summation-by-parts.

## 1. INTRODUCTION

Higher order and spectral schemes are ideally suited for resolving problems where high resolution is essential. Computational aero acoustics (CAA) and computational electro magnetics (CEM) are two such fields requiring high accuracy to resolve the vastly disparate length and time scales involved. High-order (spectral) schemes easily outperform

[1] Work funded by AFOSR 96-1-0150.



0021-9991/99 $30.00

conventional low-order schemes on simple problems, where the physical domain is smoothly mapped onto the high-order computational space. The high-order convergence rates of these schemes yield satisfactory results on relatively coarse grids.

A major difficulty in the application of high-order methods to realistic problems is the issue of applying high-order formulations to complex geometries. Often, generating a reasonable grid around a complex configuration is the most difficult aspect of the solution procedure. Further constraining grids to be smooth and higher order (necessary for high-order methods) severely complicates grid generation around complex configurations.

Many high-order practitioners advocate some form of unstructured framework. This simplifies the grid-generation procedure considerably for complex configurations. Within the context of unstructured methods there are a variety of different techniques. We choose a semistructured approach to break the geometry into piecewise smooth "subdomains," using quadrilaterals (hexahedron) in two (three) dimensions. Each subdomain is then discretized with a stable tensor product formulation, and the resulting subdomains are patched together. Notable examples of this approach include the works of Kopriva [1–3], in the context of Chebyshev spectral methods, and the works of Hesthaven [4–6], also in the context of Chebyshev methods.

Our contribution to the semistructured approach is based on an extension of the SAT method presented in [13]. It is valid for high-order finite-difference (FD) discretizations and certain spectral formulations (distinct from the works of Kopriva and Hesthaven). The SAT procedure is a **penalty** method, where the penalty parameters are determined by stability considerations or other properties of the numerical scheme. The advantages of the SAT formulation in one domain are detailed in [13] in the context of high-order FD methods. Most notably, the SAT procedure assures time stability for *systems* of equations that have a bounded energy norm. This is not true in general for other high-order FD methods. Indeed, nonpenalty approaches often lead to nonphysical growth in time for systems of equations, even though the discretization operator is stable for the scalar case [13]. Second, the SAT formulation can easily be extended to several space dimensions (via a tensor product) and to complicated boundary conditions.

In this work, we extend the SAT procedure to the case of multiple domains. We present the interface-matching conditions which maintain stability, conservation, and accuracy in multiple domains for all schemes satisfying the semidiscrete summation-by-parts convention. We note that our method (applied in a spectral context) differs from that of Kopriva [3], where the interface BC's conditions are imposed in a strong sense. In fact, we show that strong imposition of interface BC's in conjunction with FD may lead to time instabilities. We also provide a proof (missing in [4]) for stability and time stability of our approach. For simplicity, the proof is presented for the scalar one-dimensional advection–diffusion equation, but it can be easily extended to the linearized N-S equations as in [5]. Finally, we note that our approach is fully conservative. A detailed proof of the Lax–Wendroff theorem for the penalty approach will appear elsewhere.

In Section 2, we define and describe semidiscrete operators which satisfy the summation-by-parts convention, including explicit and compact finite difference schemes, as well as some spectral methods [14]. In Section 3 we present the SAT formulation for multiple domains and derive sufficient conditions for stability and time stability for the linear advection–diffusion equation. In Section 4 we derive a set of parameters that assures stability, as well as conservation for the multiple domain case. In Section 5 we present numerical examples that demonstrate the efficacy of the SAT interface procedure, as well as the inadequacy

of imposing strong interface boundary conditions. Furthermore, we show that to maintain global accuracy, interface BC's must be specified with the design accuracy of the method. Finally, we present some numerical examples specific to high-order central difference techniques. In Section 6, we present the conclusions. Finally, in the Appendix we present a detailed proof of the interface stability condition, followed by the stencils used for fourth- and sixth-order finite-difference schemes.

## 2. SPATIAL DISCRETIZATIONS

The stable interface conditions presented in this work are valid for spatial discretizations of arbitrary accuracy. To achieve this generality, the spatial discretizations must be of a specific form. Fortunately, most numerical schemes can be put into the required form with only minor modifications. To be more precise we consider discrete spatial derivative operators with the following properties:

*First-Derivative Properties*

1. The first-derivative operator defining the numerical derivative $\mathbf{u_x} = [(\partial u/\partial x)_0, \ldots, (\partial u/\partial x)_N]^{\mathrm{T}}$ is

$$\begin{aligned} P\mathbf{u_x} - Q\mathbf{u} &= 0 \\ P\mathbf{v_x} - Q\mathbf{v} &= P\mathbf{T_e}, \end{aligned} \tag{1}$$

where $\mathbf{u} = [u_0(t), u_1(t), \ldots, u_N(t)]^{\mathrm{T}}$, $\mathbf{v} = [v(x_0, t), \ldots, v(x_N, t)]^{\mathrm{T}}$, and $\mathbf{v_x} = [(\partial v/\partial x)_0, \ldots, (\partial v/\partial x)_N]^{\mathrm{T}}$. (The vector $\mathbf{v}$ is the exact solution.) The truncation error $\mathbf{T_e}$ satisfies $|\mathbf{T_e}| = O(\Delta x)^m$, where the quantity $\Delta x$ is defined as the maximum distance between any two neighboring grid points.

2. The matrix $P$ is symmetric and positive definite $(\Delta x)\, pI \le P \le (\Delta x) q I$, where $p$ and $q$ are independent of $N$ with $p > 0$ and $q > 0$.

3. The matrix $Q$ is nearly skew symmetric and satisfies the property $Q + Q^{\mathrm{T}} = D$, where the diagonal matrix $D$ has the form $d_{i,i} = [-1, 0, \ldots, 0, 1]$ for $i = 0, 1, \ldots, N$. Furthermore, $Q_{0,0} = -\frac{1}{2}$ and $Q_{N,N} = \frac{1}{2}$.

A spatial operator in the form of Eq. (1), which satisfies properties 1 through 3, is referred to as an SBP operator [7]. All SBP operators automatically lead to an energy estimate for periodic solutions to the linear advection–diffusion equation. In the finite-domain case, an energy estimate exists when an SBP operator is combined with specific boundary treatments.

Discretization operators that satisfy the SBP framework are remarkably general. Kreiss and Scherer [7] first suggested the use of SBP spatial operators in the context of second-order central-difference schemes. In Olsson [8–10] and Strand [11], high order finite difference operators are constructed, based on spatial operators of SBP type. These resulting schemes are strictly stable, which means that the growth rate of the analytic and semi-discrete solution is identical.

The precise properties of the matrices $P$ and $Q$ provide a constructive means of formulating boundary closures. A discretization begins with a parameterization of several points near the boundary of the required accuracy. The parameters are then adjusted so that they match the precise requirements of the $P$ and $Q$ matrices. Strand [12] used the

SBP approach to construct stable fourth- and sixth-order central-differencing schemes with boundary closures of the appropriate order. Carpenter, Gottlieb, and Abarbanel [13] extended the SBP formalism to compact implicit operators (fourth-order Padé operators); Carpenter and Gottlieb [14] showed that spectral formulations (Galerkin and collocation) can be cased in the SBP framework. Finally, Carpenter and Otto [15] showed that the SBP schemes have a natural interface property, and they used this property to derive a class of multiple-domain schemes referred to as "cyclo-difference" schemes. (The earlier work [15] required strong imposition of interface data, whereas the present formulation requires only weak imposition.)

The SBP schemes naturally arise with centered approximations for which the spatial operator is skew symmetric. A more general class of schemes could be formulated in the form

$$\frac{d\mathbf{u}}{dx} = P^{-1}(Q+T)\mathbf{u}, \tag{2}$$

where the matrix $T$ is symmetric negative definite. The general formulation includes the entire class of central and upwind schemes. The upwind schemes are automatically stable and accurate because they are obtained by adding a symmetric high-order diffusion operator to a stable and accurate SBP formulation. We focus, therefore, on the original SBP definition which includes central, compact, and spectral formulations.

An approach similar to that used on the first-derivative operator can be used for the second-derivative operator. For example, one can seek two positive-definite matrices $L$ and $R$ such that

$$\mathbf{v}_{xx} - L^{-1}R\mathbf{v} = O(\Delta x)^m$$

An obvious choice is to take $L = P$ and $R = QP^{-1}Q$ so that the second-derivative operator is obtained by repeated differentiation with the first-derivative operator. For spectral discretizations, differentiating the data twice with the first-derivative operator is equivalent to differentiation with an explicitly formed second-derivative operator. As such, the procedure yields an accurate representation of the second derivative (modulo roundoff errors). Repeated differentiation for finite-difference techniques is acceptable but less desirable than other, more compact formulations. A second derivative formed from two first-derivative operators is unnecessarily wide and inaccurate. The resulting stencil can produce a solution with an undamped odd–even mode. For this reason, we seek a second-derivative operator with the following properties.

*Second-Derivative Properties*

1. The second-derivative operator that defines $\mathbf{u}_{xx}$ is

$$\begin{aligned} P\mathbf{u_{xx}} - (-S^{\mathrm{T}}M + D)S\mathbf{u} &= 0 \\ P\mathbf{v_{xx}} - (-S^{\mathrm{T}}M + D)S\mathbf{v} &= P\mathbf{T_{e2}}, \end{aligned} \tag{3}$$

where the diagonal matrix $D$ has the form $d_{i,i} = [-1, 0, \ldots, 0, 1]$, $i = 0, 1, \ldots, N$.

2. The matrix $M$ is positive definite: $(\Delta x)mI \le M \le (\Delta x)nI$, where $m$ and $n$ are independent of $N$ with $m > 0$ and $n > 0$.

3. The matrix $S$ is of the form

$$S = \frac{1}{(\Delta x)} \begin{bmatrix} s_{0,0} & s_{0,1} & s_{0,2} & s_{0,3} & \cdots & & & \\ 0 & 1 & 0 & & & & & \\ & 0 & 1 & 0 & & & & \\ & & & \vdots & & & & \\ & & & 0 & 1 & 0 & & \\ & & & & 0 & 1 & 0 & \\ & & \cdots & s_{N,N-3} & s_{N,N-2} & s_{N,N-1} & s_{N,N} \end{bmatrix}, \tag{4}$$

where

$$\begin{aligned} Su|_0 &= v_x(x_0) + O(\Delta x)^r \\ Su|_N &= v_x(x_N) + O(\Delta x)^r. \end{aligned} \tag{5}$$

The matrix $S$ is the identity matrix (scaled by the grid spacing), where a discrete representation of the first derivative replaces the first and last rows.

4. The matrix $P$ is that used in the first-derivative operator.

Explicit forms of the matrices $S$ and $M$ are given in the Appendix for a second-order explicit discretization. In addition, the matrix $S$ is presented up to sixth order.

## 3. INTERFACE BOUNDARY CONDITIONS FOR MULTIPLE DOMAINS

Consider the linear advection–diffusion equation

$$\frac{\partial U}{\partial t} + a\frac{\partial U}{\partial x} = \epsilon \frac{\partial^2 U}{\partial x^2}, \quad |x| \le 1, t > 0. \tag{6}$$

Suppose that the equation is discretized by a multidomain technique such that the interval is divided arbitrarily into two subintervals $-1 \le x \le x_i$ and $x_i \le x \le 1$. On each subinterval, a discretization is used that satisfies the SBP properties 1 through 3. We propose implementing the interface boundary conditions by using a penalty treatment of the form

$$\begin{aligned} P_l \mathbf{u}_t + a Q_l \mathbf{u} &= \epsilon R_l \mathbf{u} + \sigma_1 \mathbf{e}_{\mathbf{l}i} \left( u|_{x=x_i} - v|_{x=x_i} \right) + \sigma_2 \epsilon \mathbf{e}_{\mathbf{l}i} \left[ (D_l \mathbf{u})|_{x=x_i} - (D_r \mathbf{v})|_{x=x_i} \right] \\ P_r \mathbf{v}_t + a Q_r \mathbf{v} &= \epsilon R_r \mathbf{v} + \sigma_3 \mathbf{e}_{\mathbf{r}i} \left( v|_{x=x_i} - u|_{x=x_i} \right) + \sigma_4 \epsilon \mathbf{e}_{\mathbf{r}i} \left[ (D_r \mathbf{v})|_{x=x_i} - (D_l \mathbf{u})|_{x=x_i} \right], \end{aligned} \tag{7}$$

where $\mathbf{u}$ is a vector of length $M$, $\mathbf{u} = [u_0(t), u_1(t), \ldots, u_M(t)]^{\mathrm{T}}$, defined in the left domain at the points $\mathbf{x_L} = [x_0 = -1, x_1, \ldots, x_M = x_i)]^{\mathrm{T}}$ and $\mathbf{e}_{\mathbf{l}i} = [0, \ldots, 0, 1]^{\mathrm{T}}$ is of dimension $M$. In the right domain, $\mathbf{v} = [v_0(t), v_1(t), \ldots, v_N(t)]^{\mathrm{T}}$ is defined at the points $\mathbf{x_R} = [x_0 = x_i, x_1 \ldots, x_N = 1)]^{\mathrm{T}}$ and $\mathbf{e}_{\mathbf{r}i} = [1, 0, \ldots, 0]^{\mathrm{T}}$ is of dimension $N$.

The second-derivative matrices $P_l^{-1} R_l$ and $P_r^{-1} R_r$, as well as the first-derivative matrices $P_l^{-1} Q_l$ and $P_r^{-1} Q_r$, are defined as in Section 2. The matrices $D_l$ and $D_r$ are any operators that approximate the first derivative to $O(\Delta x)^m$. The obvious first choice would be to use $P_l^{-1} Q_l$ and $P_r^{-1} Q_r$, but this choice is not essential for accuracy or stability. (In Eq. (7) we have ignored the physical boundary conditions at $x = 1$ and $x = -1$ for the sake of simplicity.)

THEOREM 3.1. *Consider the scheme* (7) *for the advection–diffusion equation* (6). *If the matrices* $P_l$, $Q_l$, $P_r$, $Q_r$, $R_l$, *and* $R_r$ *satisfy the first and second derivative properties of Section* 2 *and*

$$\sigma_3 = \sigma_1 - a, \quad \sigma_4 = \sigma_2 + 1, \quad \sigma_1 \le \frac{a}{2} - \epsilon\left[\frac{\sigma_2^2}{4\alpha_r} + \frac{\sigma_4^2}{4\alpha_l}\right], \tag{8}$$

*then* (7) *is stable.*

In the proof which follows, we have without loss of generality considered only the interface terms and ignored the terms that arise at the physical boundaries. We assume that the physical boundary conditions are implemented by stable and accurate numerical procedures. (See Hesthaven and Gottlieb [4] for a possible implementation).

*Proof.* The proof is based on a simple energy estimate. By premultiplying the equations by the vectors $\mathbf{u}^{\mathrm{T}}$ and $\mathbf{v}^{\mathrm{T}}$, respectively, and adding we obtain

$$\begin{aligned}\frac{d}{dt}\left[\|u\|_{P_l}^2 + \|v\|_{P_r}^2\right] &= 2\mathbf{u}^{\mathrm{T}}(\epsilon R_l - a Q_l)\mathbf{u} + 2\mathbf{v}^{\mathrm{T}}(\epsilon R_r - a Q_r)\mathbf{v} \\ &\quad + 2\sigma_1 u_i(u_i - v_i) + 2\epsilon\sigma_2 u_i[(D_l u)_i - (D_r v)_i] \\ &\quad + 2\sigma_3 v_i(v_i - u_i) + 2\epsilon\sigma_4 v_i[(D_r v)_i - (D_l u)_i],\end{aligned}$$

where $\|u\|_{P_l}^2 = \mathbf{u}^{\mathrm{T}} P_l \mathbf{u}$, and we have defined $u_i$, $v_i$, $(D_l u)_i$, and $(D_l v)_i$ as $u|_{x=x_i}$, $v|_{x=x_i}$, $(D_l \mathbf{u})|_{x=x_i}$, and $(D_r \mathbf{v})|_{x=x_i}$, respectively. The second-derivative properties of Section 2 lead to

$$\mathbf{u}^{\mathrm{T}} R_l \mathbf{u} \le -\alpha_l (D_l u)_i^2 + u_i (D_l u)_i \tag{9}$$

$$\mathbf{v}^{\mathrm{T}} R_r \mathbf{v} \le -\alpha_r (D_r v)_i^2 - v_i (D_r v)_i, \tag{10}$$

where the constants $\alpha_l$ and $\alpha_r$ are positive.

By using the first-derivative properties of Section 2 and Eqs. (9) and (10) and neglecting the physical boundary terms, we obtain

$$\frac{d}{dt}\left[\|u\|_{P_l}^2 + \|v\|_{P_r}^2\right] \le \mathbf{w}_i^{\mathrm{T}} B \mathbf{w}_i \tag{11}$$

where $\mathbf{w}_i = [u_i, v_i, (D_l u)_i, (D_r v)_i]$, and the interface boundary matrix $B$ is defined by

$$B = \begin{bmatrix} (-a + 2\sigma_1) & -(\sigma_1 + \sigma_3) & \epsilon(1 + \sigma_2) & -\epsilon\sigma_2 \\ -(\sigma_1 + \sigma_3) & a + 2\sigma_3 & -\epsilon\sigma_4 & \epsilon(-1 + \sigma_4) \\ \epsilon(1 + \sigma_2) & -\epsilon\sigma_4 & -2\epsilon\alpha_l & 0 \\ -\epsilon\sigma_2 & \epsilon(-1 + \sigma_4) & 0 & -2\epsilon\alpha_r \end{bmatrix}. \tag{12}$$

Straightforward (although tedious) algebra shows that conditions (8) yield a nonpositive definite matrix $B$, thus proving stability. Details are presented in Appendix I.

In practice, the values of $\sigma_1$ through $\sigma_4$ are determined as follows. The parameters $\alpha_r$ and $\alpha_l$ are functions from the numerical method and the chosen grid. The diffusion contribution in the constraint equation $\sigma_1 \le a/2 - \epsilon[\sigma_2^2/4\alpha_r + \sigma_4^2/4\alpha_l]$ is minimized for

$\sigma_2 = -\alpha_r/(\alpha_r + \alpha_l)$, yielding the expression $\sigma_1 \le a/2 - \epsilon[1/4(\alpha_r + \alpha_l)]$. The value $\sigma_1$ determines the dissipation at the interface and also influences the effective CFL of the numerical scheme. Values of $\sigma_1$ in the range $-1 \le \sigma_1 \le 0$ provide a compromise between adequate levels of dissipation and acceptable numerical efficiency.

We have shown that the linking of two domains at an interface with the interface conditions prescribed in Theorem 3.1 is stable in a semidiscrete sense for specific values of the penalty parameters $\sigma_1$ through $\sigma_4$. The basic methodology can be extended to an arbitrary number of subdomains without complication. The only constraint is that the numerical method must satisfy the SBP framework. The methodology does not rely on subdomain size and does not require the same SBP operator to be used in each domain. In principle, a finite-difference operator of any order, as well as spectral operators on subdomains of arbitrary size, can be linked together in a stable manner. Practical details on how to chose $\sigma_1$ through $\sigma_4$ are included in the results section (Section 6).

In Section 2, we presented the general form of second-derivative operators appropriate for this work. We then noted two specific derivative operators that satisfy this form. We now show that both choices for the matrices $R_l$ (and $R_r$) suggested in Section 2 satisfy conditions (9) and (10) of Theorem 3.1. We start with the first option (i.e., $R_l = Q_l P_l^{-1} Q_l$). In this case, the first derivative matrix in (7) is $D_l = P_l^{-1} Q_l$. Thus, the quantity $\mathbf{u}^{\mathrm{T}} R_l \mathbf{u}$ becomes

$$\begin{aligned}\mathbf{u}^{\mathrm{T}} Q_l P_l^{-1} Q_l \mathbf{u} &= \mathbf{u}^{\mathrm{T}} Q_l P_l^{-1} P_l P_l^{-1} Q_l \mathbf{u} \\ &= -\left(P_l^{-1} Q_l \mathbf{u}\right)^{\mathrm{T}} P_l \left(P_l^{-1} Q_l \mathbf{u}\right) + u_i \left(P_l^{-1} Q_l u\right)_i,\end{aligned}$$

where we have used the SBP property $Q + Q^{\mathrm{T}} = D$ and have ignored the physical boundary contribution.

We recall now that $P_l \ge (\Delta x)\, p_l$ so that

$$\begin{aligned}\mathbf{u}^{\mathrm{T}} R_l \mathbf{u} &= \mathbf{u}^{\mathrm{T}} Q_l P_l^{-1} Q_l \mathbf{u} \\ &\le -(\Delta x)\, p_l |(D_l \mathbf{u})|^2 + u_i (D_l u)_i.\end{aligned}$$

Thus, (9) is satisfied with $\alpha_l = (\Delta x)\, p_l$. A similar result holds for $R_r$ with $\alpha_r = (\Delta x)\, p_r$.

The second choice presented in Section 2 for the second-derivative operator $P^{-1} R_l$ is of the form of Eq. (3):

$$P^{-1} R_l = P^{-1}(-S^T M + D) S.$$

For the purpose of proving stability, we relate the two matrices $D_l = S$ (in actuality, only the first and last rows satisfy $D_l = S$; they are, however, the only portions of the matrices that enter the proof):

$$\begin{aligned}\mathbf{u}^{\mathrm{T}} R_l \mathbf{u} &= -(S\mathbf{u})^T M S\mathbf{u} + U_i (S\mathbf{u})_i \\ &\le -(\Delta x) m |S\mathbf{u}|^2 + U_i (S\mathbf{u})_i.\end{aligned}$$

Thus, (9) is satisfied with $\alpha_l = (\Delta x) m$.

## 4. CONSERVATION AT THE INTERFACE

The Lax–Wendroff theorem [16] addresses the complexities encountered in solving nonlinear conservation laws. The theorem states that a convergent numerical approximation

$U_l(x,t)$, computed with a consistent and *conservative* method, converges to a weak solution of the conservation law. Note that discrete conservation is necessary to satisfy the conditions of the theorem.

A heuristic definition of conservation (commonly encountered by practitioners) describes how the numerical flux function "telescopes" across a domain to the boundaries. The total quantity of a conserved variable in any region changes only as a result of the flux through the boundaries of the region. We, however, rely on a broader definition of conservation motivated by the original proof of the Lax–Wendroff theorem. We demand that the numerical flux telescope across the domain and that all moments of the flux against an arbitrary test function telescope across the domain. This additional constraint demands an equivalence between the weak forms of the continuous and discrete operators.

We begin by discussing conservation in a single domain. Consider the nonlinear equation $U_t + F_x = 0$ on $-1 \le x \le 1$ and $t \ge 0$. Note that in the linear case, $F = aU$ and we obtain (6) with $\epsilon = 0$. To obtain the weak form of this equation we multiply by an arbitrary test function $\phi(x,t)$ that vanishes on the boundaries. By integrating with respect to space and time we obtain an integral statement of the original differential equation:

$$\int_{-1}^{1} \phi U \, dx \Big|_0^t - \int_0^t \int_{-1}^{1} (U\phi_t + F\phi_x) \, dx \, d\tau = 0.$$

Now consider the semidiscrete equation given by $P\mathbf{U}_t + Q\mathbf{F} = 0$. Here, we have replaced the spatial derivative $F_x$ in the continuous case with an SBP derivative operator of order $(\Delta x)^r$. By multiplying by the discrete vector $\phi(x_j) = \phi^{\mathrm{T}}$ (the discrete analog of integration) and integrating with respect to time, we obtain

$$\phi^{\mathrm{T}} P U \Big|_0^t - \int_0^t \left( U^{\mathrm{T}} P \phi_t + F^{\mathrm{T}} Q \phi \right) d\tau = 0.$$

Thus, the semidiscrete operator satisfies a weak form similar to that of the continuous operator and asymptotically approaches the continuous operator in the limit of infinite spatial resolution. The special form of the $P$ and $Q$ matrices present in the SBP operators enables the semidiscrete operator to mimic the conservation property of the continuous operator.

The equivalence between the continuous and semidiscrete operators is more complicated for multiple domains. The conservation property of the SBP operator does not necessarily apply at an interface boundary. Under very mild restrictions, however, the SBP interface operators telescope out to the physical boundaries, as does the continuous operator. Because conservation is only necessary for the advection terms in the advection–diffusion equation, we set $\epsilon = 0$ (see Eq. (6)) and prove conservation for a two-domain discretization. We prove conservation for a general nonlinear flux. Note that the penalty parameters for this nonlinear case are designated $\hat{\sigma}_1$ and $\hat{\sigma}_3$. The resulting conservation condition obtained in the nonlinear case is slightly different from that obtained in the linear analysis. This difference results from different scalings of the penalty parameters.

THEOREM 4.1. *Assume the nonlinear equation* $\partial U/\partial t + \partial F(U)/\partial x = 0$ *is valid on the interval* $-1 \le x \le 1$, $t > 0$, *divided arbitrarily into two subintervals* $-1 \le x \le x_i$ *and*

$x_i \le x \le 1$. *On each subinterval, a discretization is used that satisfies the SBP framework, and boundary conditions are imposed via penalties in the form*

$$\begin{aligned} \mathbf{u}_t + P_l^{-1} Q_l \mathbf{F}(\mathbf{u}) &= \hat{\sigma}_1 P_l^{-1} \mathbf{e}_{\mathbf{l}i} [F(u(x_i)) - F(v(x_i))] \\ \mathbf{v}_t + P_r^{-1} Q_r \mathbf{F}(\mathbf{v}) &= \hat{\sigma}_3 P_r^{-1} \mathbf{e}_{\mathbf{r}i} [F(v(x_i)) - F(u(x_i))], \end{aligned} \tag{13}$$

*where* $\mathbf{u} = [u_0(t), u_1(t), \ldots, u_M(t)]^{\mathrm{T}}$ *is defined in the left domain at the points* $\mathbf{x}_{\mathbf{L}} = [x_0 = -1, x_1, \ldots, x_M = x_i]^{\mathrm{T}}$ *and* $e_{\mathbf{l}i} = [0, \ldots 0, 1]^{\mathrm{T}}$ *is of dimension M with similar definitions on the right domain. The discretization is conservative provided that the stability condition* $\hat{\sigma}_3 = \hat{\sigma}_1 - 1$ *is satisfied.*

*Proof.* For multiple domains, we proceed as shown previously in the single-domain case. Multiplying Eqs. (13) by the vectors $\phi^{\mathrm{T}} P_l$ and $\phi^{\mathrm{T}} P_r$, respectively, yields the set of equations

$$\begin{aligned} \phi^{\mathrm{T}} P_l \mathbf{u}_t + \phi^{\mathrm{T}} Q_l \mathbf{F}(\mathbf{u}) &= \hat{\sigma}_1 \phi(x_i)(F(u(x_i)) - F(v(x_i))) \\ \phi^{\mathrm{T}} P_r \mathbf{v}_t + \phi^{\mathrm{T}} Q_r \mathbf{F}(\mathbf{v}) &= \hat{\sigma}_3 \phi(x_i)(F(v(x_i)) - F(u(x_i))). \end{aligned}$$

Using the properties of $Q_l$ and $Q_r$ we get

$$\begin{aligned} \phi^{\mathrm{T}} P_l \mathbf{u}_t - \mathbf{F}^{\mathrm{T}} Q_l \phi + \phi(x_i) F(u(x_i)) &= \hat{\sigma}_1 \phi(x_i)(F(u(x_i)) - F(v(x_i))) \\ \phi^{\mathrm{T}} P_r \mathbf{v}_t - \mathbf{F}^{\mathrm{T}} Q_r \phi - \phi(x_i) F(v(x_i)) &= \hat{\sigma}_3 \phi(x_i)(F(v(x_i)) - F(u(x_i))). \end{aligned}$$

By integrating with respect to time and making use of the fact that $\phi$ is continuous at the interface, we get

$$\begin{aligned} \phi^{\mathrm{T}} P_l \mathbf{u}|_0^t + \phi^{\mathrm{T}} P_r \mathbf{v}|_0^t = &\int_0^t \left( \mathbf{u}^{\mathrm{T}} P_l \phi_t + \mathbf{F}^{\mathrm{T}} Q_l \phi \right) d\tau + \int_0^t \left( \mathbf{v}^{\mathrm{T}} P_r \phi_t + \mathbf{F}^{\mathrm{T}} Q_r \phi \right) d\tau \\ &+ \int_0^t \phi_i F(u(x_i))(\hat{\sigma}_1 - \hat{\sigma}_3 - 1)\, d\tau \\ &+ \int_0^t \phi_i F(v(x_i))(\hat{\sigma}_3 - \hat{\sigma}_1 + 1)\, d\tau. \end{aligned}$$

Obviously, the condition $\hat{\sigma}_3 = \hat{\sigma}_1 - 1$ eliminates the interface terms from the expression and leaves the desired weak form of the semidiscrete equation. Thus, the theorem is proved.

## 5. COMPUTATIONAL RESULTS

In this section we present numerical results that demonstrate the efficacy of the methodology presented in this paper. We begin by showing that the new interface boundary conditions ensure stability, while conventional interface treatments do not. We next show that one can sacrifice, locally, one degree of accuracy when constructing the derivative matrices $P$, $Q$, and $R$ (see Eq. (7)) but not when approximating the matrices $D_l$ and $D_r$. Finally, we present a multidomain test case showing the capabilities of the new interface methodology.

*Stability*

We begin by justifying for the use of the SAT boundary conditions. Reference [13] details the advantages of the SAT procedure for a single domain, noting that the principle advantage is the guarantee of stability and time stability for the constant coefficient hyperbolic system. All conventional boundary closures for fourth- or sixth-order central/compact schemes (no proof, just empirical evidence) lead to *system* energy growth in time, despite time stability for the scalar hyperbolic equation $U_t + U_x = 0$. Thus, the SAT procedure and the projection method [9, 10] are the only know mechanisms for ensuring time stability for long time integrations of systems of hyperbolic equations for high-order central FD methods.

The following test problem was used in Ref. [13] to demonstrate the time stability of the SAT procedure:

$$\begin{aligned} \frac{\partial u}{\partial t} + \frac{\partial u}{\partial x} &= 0, \\ \frac{\partial v}{\partial t} - \frac{\partial v}{\partial x} &= 0, \quad 0 \le x \le 1, t \ge 0; \end{aligned} \tag{14}$$

$$u(0,t) = \alpha v(0,t), \quad v(1,t) = \beta u(1,t), \quad t \ge 0, \tag{15}$$

$$u(x,0) = \sin 2\pi x, \quad v(x,0) = -\sin 2\pi x, \quad 0 \le x \le 1. \tag{16}$$

For reflection coefficients $\alpha$ and $\beta$ satisfying $|\alpha\beta| < 1$, the solution decays in time, whereas if $|\alpha\beta| > 1$, the solution grows in time. The case $|\alpha\beta| = 1$ is neutrally time stable (the $L^2$ norm of the solution remains constant in time) and provides an *extremely* severe test of the time stability of a numerical method. All conventional boundary procedures display nonphysical growth in time as $|\alpha\beta| \to 1$. In addition, merely satisfying the summation by parts convention for the boundary closure is not sufficient to guarantee time stability. Both the summation by parts convention and an SAT boundary imposition (or a projection method) are necessary to ensure time stability for systems of equations [13].

We now extend this analysis to the multiple domain context using Eq. (14) as our test case. Rather than determining time stability by directly integrating Eq. (14) to long times, we focus on eigenvalue analysis of the semidiscrete system. (In [13], an equivalence is established between the two procedures. Specifically, eigenvalues with positive real parts yield solutions that exhibit nonphysical grow in time.) Figure 1 shows the eigenvalues from the system study using the sixth-order explicit method. The domain is discretized using 97 equally spaced points, arranged into 1, 2, 4, and 8 subdomains. The values $\alpha = \beta = 1$ are used, corresponding to the neutrally stable case for which the solution is $u(x,t) = \sin 2\pi(x-t)$, $v(x,t) = -\sin 2\pi(x+t)$, $0 \le x \le 1$, $t \ge 0$. All eigenvalues are confined to the left-half plane. Experimental tests for the case $\alpha = \beta = 1 - \epsilon$ confirm that the rightmost eigenvalue approaches the imaginary axis linearly as the variable $\epsilon \to 0$. Similar results are obtained for the fourth-order spatial operator. Thus, the fourth- and sixth-order schemes are time stable, independent of the number of subdomains.

Conversely, Fig. 2 shows the eigenvalues resulting from a conventional imposition of the interface conditions. (For increased clarity only the 8-subdomains case is shown. Similar

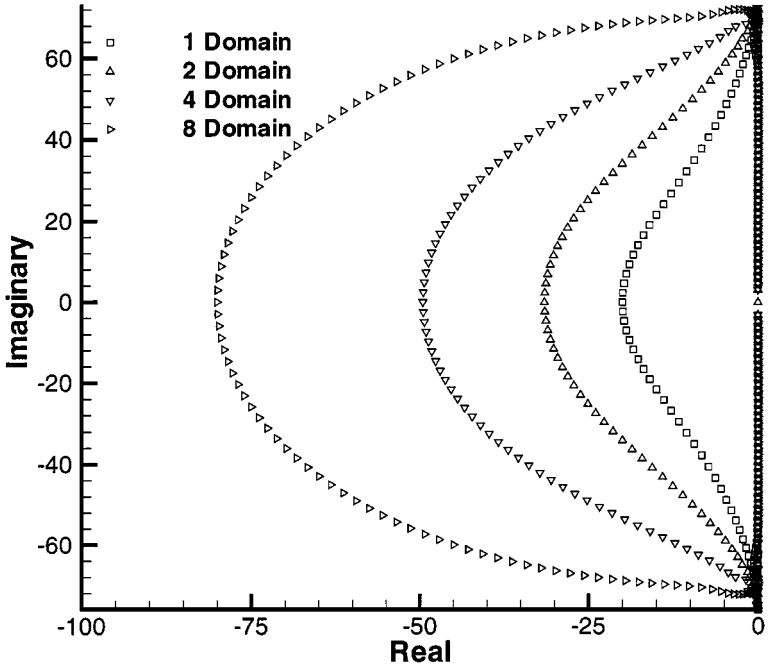


**FIG. 1.** Eigenvalues for the hyperbolic system discretized with a sixth-order scheme and the new interface conditions.

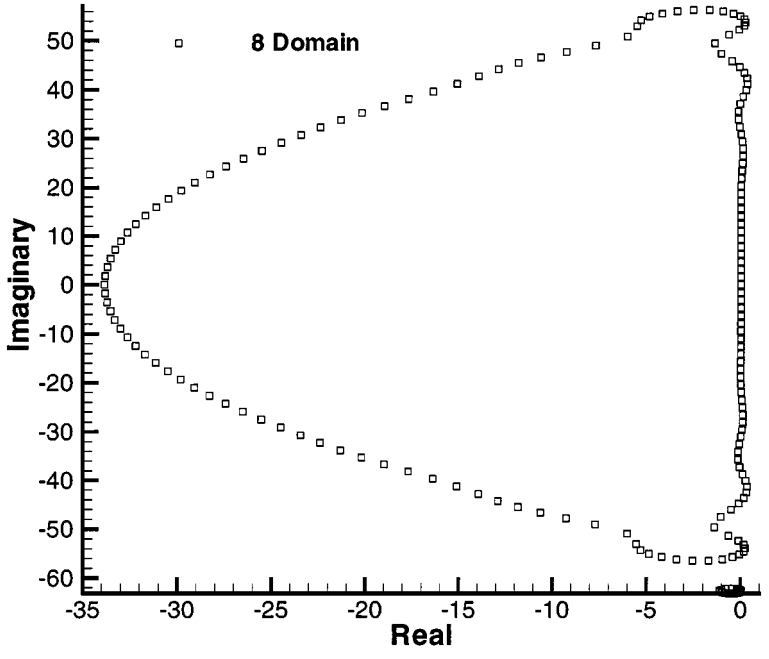


**FIG. 2.** Eigenvalues for the hyperbolic system discretized with a sixth-order scheme and conventional upwind interface conditions.

**TABLE I**
**$L_2$ Reflection Coefficient Required to Maintain Negative Eigenvalues**

| Domains | $\alpha$ |
|---|---|
| 1 | 1.0 |
| 2 | 0.86 |
| 4 | 0.60 |
| 6 | 0.42 |
| 8 | 0.30 |

results are obtained with 2, 4, and 6 subdomains.) The interface condition is obtained by choosing the upwind value from the left and right interface state for the left-moving and right-moving characteristic functions. (Note that we do not have a proof of conservation for this procedure.) The physical boundary conditions at $x = 0$ and $x = 1$ are imposed via the SAT procedure to eliminate the obvious single domain instability shown to exist in Ref. [13]. The "upwind" eigenspectrum has many eigenvalues in the right-half plane and, thus, will exhibit growth in time of the solution. To quantify the nature of this interface instability, Table I shows a parametric study in $\alpha = \beta$, identifying the maximum value of $\alpha$ for which time stability can be ensured. Note that as the number of interfaces increases the system requires more dissipation (smaller reflection coefficients $\alpha$ and $\beta$) to ensure time stability.

This example demonstrates that the new interface boundary conditions are time stable for the constant coefficient hyperbolic system given by Eq. (14). In addition, inappropriate treatment of interface boundaries are shown to generate instabilities for systems of equations. As with the single domain, a summation-by-parts boundary closure, in conjunction with an SAT penalty treatment for the physical boundary conditions, provides system stability, where conventional interface treatments failed.

*Accuracy: Single Domain*

A significant obstacle in dealing with high-order finite-difference schemes is the formulation of stable stencils near the boundaries. A uniformly high-order approximation should be used if possible. In most high-order formulations, however, ensuring uniform accuracy up to the boundaries is difficult while maintaining numerical stability. Fortunately, the work of Gustafsson [17] shows that design accuracy (the designed order of accuracy $p$) is achieved in advection–diffusion equations, even if a finite number of points (independent of $N$) are closed with stencils that are less accurate by one order. Thus, a $p$th-order interior discretization will asymptotically achieve $p$th-order $L_2$ accuracy with $(p-1)$th-order closures near the boundaries.

Another concern pertaining to numerical accuracy, is the effect of imposing inaccurate boundary conditions. In a numerical simulation, it is often impossible to obtain exact physical boundary data. It is well known that imposing approximate boundary data reduces the accuracy of the solution, if the data is less accurate than the design order of the numerical method. What is not clear, however, is the overall impact of interface boundaries on global solution accuracy.

To address these issues, we consider an advection–diffusion problem, first in a single domain and then in multiple domains. The nonlinear Burgers' equation is used,

$$\frac{\partial U}{\partial t} + U\frac{\partial U}{\partial x} = \epsilon\frac{\partial^2 U}{\partial x^2}, \quad -1 \le x \le 1; t > 0, \tag{17}$$

with the exact solution

$$U(x,t) = -a\tanh\left(a\frac{x-ct}{2\epsilon}\right) + c, \quad -\infty < x < \infty; t < 0. \tag{18}$$

The solution of (17) requires imposition of boundary conditions at each end of the physical domain. We choose Robin boundary conditions of the form

$$\alpha u(-1,t) - \beta\frac{\partial u}{\partial x}\bigg|_{-1} = g_{-1}(t), \quad \gamma u(1,t) - \delta\frac{\partial u}{\partial x}\bigg|_{1} = g_1(t).$$

We consider the scheme

$$PU_t = -Q\left(\frac{1}{2}U^2\right) + \epsilon RU + \tau_1[\alpha U(-1) - \beta(DU)(-1)] + \tau_2[\gamma U(1) - \delta(DU)(1)], \tag{19}$$

where the matrices $P$, $Q$, $R$ satisfy the summation by parts conditions, and the matrix $D$ is an approximation to the first derivative. The time-advancement scheme is a five-stage fourth-order low-storage Runge–Kutta scheme. The time step is chosen to ensure that the temporal error in the formulation is small relative to the spatial error. The simulation is run to a physical time of $T = 1$, and the viscosity is determined by the value $\epsilon = 5 \times 10^{-1}$.

At issue is the order of accuracy required in the construction of $P$, $Q$, $R$, and $D$ to maintain design solution accuracy. We show that for design accuracy $p$, the matrices $P^{-1}Q$ and $P^{-1}R$ can be of order $p-1$ locally, whereas the matrix $D$ has to approximate the first derivative to order $p$. This is not surprising since for stability $\tau_1$ and $\tau_2$ are of order $1/\Delta x$, which, when combined with boundary data terms of design accuracy $p$, yield local errors of order $p-1$. Thus, the physical boundary conditions imposed with design accuracy $p$ and local boundary closures of order $p-1$ have a similar impact on the global norm of the error.

Tables II and III present a grid-refinement study on a single domain. Table II presents a refinement study comparing boundary closures of various accuracy. The classical fourth-order explicit scheme is used in all cases in the domain interior, while the boundaries

**TABLE II**

**$L_2$ Solution Errors: Convergence Rate of "Fourth-Order" Schemes**

| | (4,4-4-4,4) | | (3,3-4-3,3) | | (2,2-4-2,2) | |
|---|---|---|---|---|---|---|
| $N$ | $\text{Log}_{10}$ error | Rate | $\text{Log}_{10}$ error | Rate | $\text{Log}_{10}$ error | Rate |
| 33 | −3.847 | | −3.694 | | −2.974 | |
| 65 | −4.082 | 2.31 | −4.797 | 3.66 | −4.074 | 3.65 |
| 129 | −5.239 | 3.84 | −5.971 | 3.90 | −5.519 | 4.80 |
| 257 | −6.486 | 4.14 | −6.117 | 3.81 | −6.284 | 2.54 |
| 513 | −7.731 | 4.14 | −7.276 | 3.85 | −7.048 | 2.54 |
| 1025 | −8.960 | 4.87 | −9.455 | 3.92 | −7.898 | 2.82 |

**TABLE III**
**$L_2$ Solution Errors: Convergence Rate of Uniformly Fourth-Order Scheme Using Third-Order Accurate Boundary Conditions**

| $N$ | $\text{Log}_{10}$ error | Rate |
|---|---|---|
| 33 | −3.004 | |
| 65 | −4.002 | 3.32 |
| 129 | −4.764 | 2.53 |
| 257 | −5.636 | 2.90 |
| 513 | −6.531 | 2.97 |
| 1025 | −7.898 | 2.82 |

are closed with stencils of order 4, 3, and 2, respectively. We refer to these schemes as (4,4-4-4,4), (3,3-4-3,3), and (2,2-4-2,2). The derivative term $D$ in the Robins' boundary conditions is approximated to $O(\Delta x^4)$ in all cases. We note that the convergence rate in Table II is fourth order for the (4,4-4-4,4) and (3,3-4-3,3) schemes, and third order for the (2,2-4-2,2) scheme. For the (3,3-4-3,3) scheme, both the advection and diffusion stencils are reduced by one order of accuracy near the boundaries. We note that the convergence rate asymptotes to fourth order and that the absolute levels of error are comparable to those obtained using the (4,4-4-4,4) scheme. The (2,2-4-2,2) scheme is second order locally at each boundary and fourth order in the interior. (Only the diffusion terms are treated with second-order accuracy near the boundaries, while the advection terms are treated with third-order accuracy. Thus, any degradation in accuracy results from approximating the diffusion terms.) We note that the convergence rate for this case asymptotes to third order, which is a reduction in global accuracy by one order. This behavior is consistent with Gustafsson's [17] theory, specifically, that global solution accuracy allows a finite number of stencils to be reduced by one order of accuracy.

Table III shows the final study, in which the advection and diffusion stencils ($P^{-1}Q$ and $P^{-1}R$) are uniformly fourth-order accurate (4,4-4-4,4). The physical boundary condition (including the matrix $D$) is approximated to $O(\Delta x^3)$. The convergence rate in Table III asymptotes to third order, which is a reduction in global accuracy by one order.

This series of tests on the single domain indicates the need to impose the *physical* boundary conditions with design accuracy. However, closing the near boundary stencils with an accuracy that is one order less than the design interior accuracy appears to be sufficient.

*Accuracy: The Multidomain Case*

We now demonstrate by numerical example that these results generalize to the case of multiple domains. Table IV shows a grid-refinement study that compares one and eight spatial domains. The numerical test problem is the previously described Burgers' equation using a value of $\epsilon = 10^{-2}$. The equation is discretized as in (7) and the numerical scheme used in both cases is the (3,3,3,3-4-3,3,3,3) SAT scheme with physical boundary conditions (i.e., the matrices $D_l$ and $D_r$ approximate the first derivative to an accuracy of $O(\Delta x^4)$. We note that the convergence rate in Table IV asymptotes to fourth order for both the one- and eight-domain cases.

**TABLE IV**
**$L_2$ Solution Errors: Convergence Rate of Fourth-Order Scheme with Third-Order Closure at Interfaces on Multiple Domain Problem**

| | 1 domains | | 8 domains | |
|---|---|---|---|---|
| $N$ | $\text{Log}_{10}$ error | Rate | $\text{Log}_{10}$ error | Rate |
| 97 | −2.148 | | −2.125 | |
| 193 | −3.016 | 2.88 | −3.143 | 3.38 |
| 385 | −4.214 | 3.98 | −4.485 | 4.45 |
| 769 | −5.372 | 3.85 | −5.656 | 3.38 |
| 1537 | −6.505 | 3.76 | −6.866 | 4.02 |
| 3063 | −7.664 | 3.85 | −8.055 | 3.95 |

Another example that directly compares the effects of boundary condition accuracy is presented in Table V, using Burgers' equation ($\epsilon = 10^{-2}$) as the test problem. The sixth-order SAT scheme (5,5,5,5,5,5-6-5,5,5,5,5) is used for the spatial discretization operator, and the interval $-1 \leq x \leq 1$ is divided into eight even subdomains. The physical boundary conditions and interface conditions ($D_l$ and $D_r$) are constructed to approximate the first derivative to an accuracy of either $O(\Delta x^6)$ and $O(\Delta x^5)$. Thus, the formal accuracy of each scheme is sixth- and fifth-order, respectively. Table V compares the solution accuracy obtained with the two schemes. The convergence rates (based on the last four refinements) are 5.45 and 4.17, respectively. As predicted, both schemes asymptotically converge at their theoretical rates.

These examples demonstrate that design accuracy is achieved with multiple domains if the physical boundary conditions are imposed with design accuracy and the numerical closures near the interfaces are at most one order of accuracy less than the design accuracy of the interior scheme.

*Nonuniform Domain*

The final problem we solve is the nonlinear Burgers' equation with unequally spaced subdomains and a sixth-order scheme. Details of the numerical discretization are included in the Appendix. The Burgers' equation in the form of Eq. (17) is solved throughout the domain with a viscosity parameter of $\epsilon = 10^{-2}$. The domain is divided into 12 subdomains, each

**TABLE V**
**$L_2$ Solution Errors: Dependence on Interface Closures for Sixth-Order Scheme**

| | Sixth-order | | Fifth-order | |
|---|---|---|---|---|
| $N$ | $\text{Log}_{10}$ error | Rate | $\text{Log}_{10}$ error | Rate |
| 97 | −2.357 | | −2.234 | |
| 193 | −3.339 | 3.26 | −3.366 | 3.76 |
| 385 | −4.766 | 4.74 | −4.135 | 2.55 |
| 769 | −6.718 | 6.48 | −6.158 | 6.72 |
| 1537 | −8.257 | 5.11 | −7.022 | 2.87 |
| 3063 | −9.898 | 5.45 | −8.392 | 4.55 |

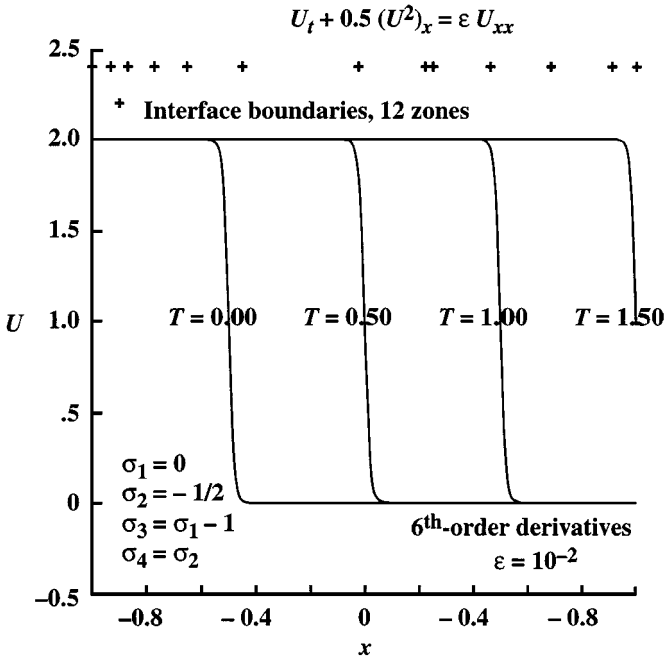


**FIG. 3.** The Burgers equation solved using a sixth-order scheme with randomly generated interface points.

with the same number of points and a uniform local discretization. The domain interfaces are placed randomly on the interval $-1 \le x \le 1$. The ratio of maximum to minimum subdomain size is about 15:1. Figure 3 shows the solution at four different times. The "symbols" at the top of the figure show the positions of the 11 interface points. The profiles are smooth and monotone for this discretization. Figure 4 shows the logarithm of the solution error plotted as a function of space on the sequence of five grids.

This problem demonstrates the stability and accuracy of the new interface treatments. The discretization asymptote to a convergence rate of sixth order on the sequence of grids. Table VI shows the convergence rate of the calculations, for two different values of the parameter $\epsilon$. The steep gradients are resolved to high-order on all grids for $\epsilon = 10^{-2}$. For $\epsilon = 2 \times 10^{-3}$, the two coarsest grids are not yet achieving high-order accuracy, and two-point grid oscillations exist in the solution. Further reduction of $\epsilon$ causes numerical instability,

**TABLE VI**

**$L_2$ Solution Errors: Convergence of Sixth-Order Scheme with 12 Subdomains and Interfaces Distributed Randomly**

| | $\epsilon = 10^{-2}$ | | $\epsilon = 2 \times 10^{-3}$ | |
|---|---|---|---|---|
| $N$ | $\text{Log}_{10}$ error | Rate | $\text{Log}_{10}$ error | Rate |
| 145 | −3.090 | | −1.376 | |
| 289 | −4.641 | 5.15 | −1.865 | 1.62 |
| 577 | −5.915 | 4.22 | −3.053 | 3.95 |
| 1153 | −7.520 | 5.33 | −4.574 | 5.05 |
| 2305 | −9.370 | 6.15 | −5.834 | 4.18 |

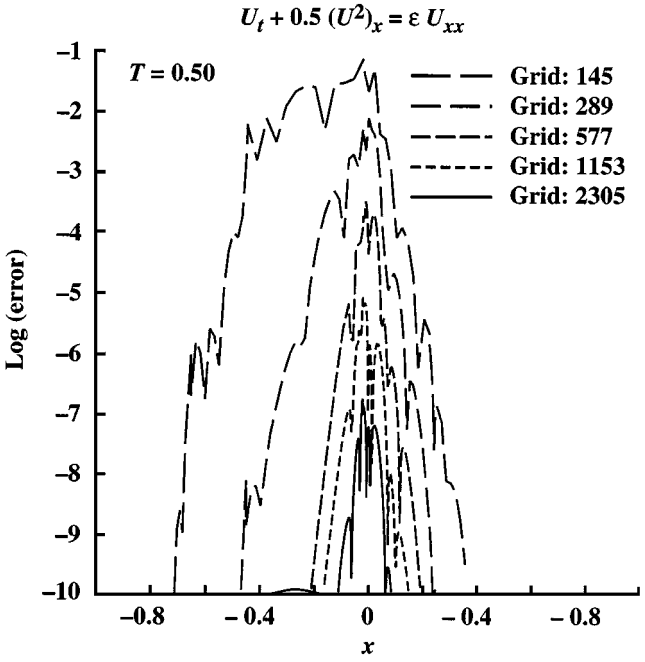


**FIG. 4.** Errors obtained from Burgers equation solved on a sequence of grids with a sixth-order scheme.

emanating from the interface location, as the gradients pass the interface. Increasing the robustness of the interface conditions for marginally resolved/discontinuous cases is the focus of current research.

## 6. CONCLUSIONS

We focus on high-order finite difference schemes, which satisfy the summation-by-parts (SBP) discretization framework. We show stable and conservative interface treatments of arbitrary spatial accuracy for the linear advection–diffusion equation. Problems with multiple domains and abruptly changing mesh sizes are considered.

Finite-difference operators are shown to admit design accuracy ($p$th-order global accuracy) when $(p-1)$th-order stencil closures are used near boundaries if the "physical" boundary conditions (and interface conditions) are imposed with $p$th-order accuracy. Finite-difference operators of up to sixth order are constructed which satisfy the constraints of the new interface procedures.

Accurate sixth-order calculations are achieved for the nonlinear Burgers equation on a 12-subdomain problem having randomly distributed interfaces.

## APPENDIX I: STABILITY

Here we show the algebra involved in proving Theorem 3.1. We begin by restating of the stability condition presented in Eq. (11) governing the total energy of the system,

$$\frac{d}{dt}\left[\|u\|^2_{P_l} + \|v\|^2_{P_r}\right] \le \mathbf{w}_i^{\mathrm{T}} B \mathbf{w}_i, \tag{20}$$

where $\mathbf{w}_i = [u_i, v_i, (D_l u)_i, (D_r v)_i]$, and the boundary matrix defined in Eq. (12) is defined by

$$B = \begin{bmatrix} (-a+2\sigma_1) & -(\sigma_1+\sigma_3) & \epsilon(1+\sigma_2) & -\epsilon\sigma_2 \\ -(\sigma_1+\sigma_3) & a+2\sigma_3 & -\epsilon\sigma_4 & \epsilon(-1+\sigma_4) \\ \epsilon(1+\sigma_2) & -\epsilon\sigma_4 & -2\epsilon\alpha_l & 0 \\ -\epsilon\sigma_2 & \epsilon(-1+\sigma_4) & 0 & -2\epsilon\alpha_r \end{bmatrix}. \tag{21}$$

The stability of this matrix is easier to analyze if it is rotated with a similarity transformation. Define the new vector $\hat{\mathbf{w}} = S\mathbf{w}$ such that

$$\hat{\mathbf{w}} = \frac{1}{\sqrt{2}} \begin{bmatrix} u_i - v_i \\ u_i + v_i \\ (D_l u)_i - (D_r v)_i \\ (D_l u)_i + (D_r v)_i \end{bmatrix} = \frac{1}{\sqrt{2}} \begin{bmatrix} 1 & -1 & 0 & 0 \\ 1 & 1 & 0 & 0 \\ 0 & 0 & 1 & -1 \\ 0 & 0 & 1 & 1 \end{bmatrix} \begin{bmatrix} u_i \\ v_i \\ (D_l u)_i \\ (D_r v)_i \end{bmatrix}. \tag{22}$$

The similarity rotation matrix has the property $S^{\mathrm{T}} = S^{-1}$ as can easily be verified. The rotation matrix $S$ can be used to transform the stability condition defined by Eq. (11) into the equivalent condition:

$$\mathbf{w}_i^{\mathrm{T}} M^i \mathbf{w}_i = \mathbf{w}_i^{\mathrm{T}} S^{\mathrm{T}} S M^i S^{\mathrm{T}} S \mathbf{w}_i = \hat{\mathbf{w}}^{\mathrm{T}} \hat{M}^i \hat{\mathbf{w}} \le 0, \tag{23}$$

where

$$\hat{M}^i = \begin{bmatrix} 2(\sigma_1+\sigma_3) & -(-\sigma_1+\sigma_3+a) & \epsilon(\sigma_2+\sigma_4) & \epsilon \\ -(-\sigma_1+\sigma_3+a) & 0 & -\epsilon(-\sigma_2+\sigma_4-1) & 0 \\ \epsilon(\sigma_2+\sigma_4) & -\epsilon(-\sigma_2+\sigma_4-1) & -\epsilon(\alpha_r+\alpha_l) & \epsilon(\alpha_r-\alpha_l) \\ \epsilon & 0 & \epsilon(\alpha_r-\alpha_l) & -\epsilon(\alpha_r+\alpha_l) \end{bmatrix}. \tag{24}$$

To ensure negative definiteness, every submatrix in the matrix $\hat{M}^i$ must be negative definite. We observe by inspection that $(\sigma_1+\sigma_3) \le 0$ is a necessary condition. Analyzing the $2\times 2$ submatrices along the diagonal, we obtain the necessary conditions $(-\sigma_1+\sigma_3+a) = 0$ and $\epsilon(-\sigma_2+\sigma_4-1) = 0$. Substituting the equalities $(-\sigma_1+\sigma_3+a) = 0$ and $(-\sigma_2+\sigma_4-1) = 0$ into the matrix $\hat{M}^i$ yields

$$\hat{M}^i = \begin{bmatrix} 2(2\sigma_1-a) & 0 & \epsilon(2\sigma_2+1) & \epsilon \\ 0 & 0 & 0 & 0 \\ \epsilon(2\sigma_2+1) & 0 & -\epsilon(\alpha_r+\alpha_l) & \epsilon(\alpha_r-\alpha_l) \\ \epsilon & 0 & \epsilon(\alpha_r-\alpha_l) & -\epsilon(\alpha_r+\alpha_l) \end{bmatrix}. \tag{25}$$

A symmetric matrix can be rotated into diagonal form by an orthogonal matrix, making the condition of negative semi-definiteness

$$\hat{\mathbf{w}}^{\mathrm{T}} \hat{U}^{\mathrm{T}} D^i \hat{U} \hat{\mathbf{w}} \le 0,$$

where $\hat{U}$ is the orthogonal matrix that satisfies $\hat{U}^{\mathrm{T}} D^i \hat{U} = \hat{M}^i$. Pre- and postmultiplication of $\hat{M}^i$ by suitable rotation matrices $M_\lambda = R_1^{\mathrm{T}} \hat{M}^i R_1$ yield the equivalent condition

$$\hat{\mathbf{w}}^{\mathrm{T}} R_1^{\mathrm{T}} \hat{U}^{\mathrm{T}} D^i \hat{U} R_1 \hat{\mathbf{w}} \le 0.$$

The matrix $R_1$, chosen to yield a diagonal expression for the matrix $M_\lambda$ is

$$L_1 = \begin{bmatrix} 1 & 0 & 0 & 0 \\ 0 & 1 & 0 & 0 \\ L_{3,1} & 0 & 1 & 0 \\ L_{4,1} & 0 & L_{4,3} & 1 \end{bmatrix} \tag{26}$$

with

$$\begin{aligned} L_{3,1} &= \frac{-\epsilon(2\sigma_2+1)}{2(2\sigma_1-a)} \\ L_{4,1} &= \frac{-2\epsilon(\alpha_r\sigma_2-\alpha_l\sigma_2+\alpha_r)}{\epsilon\left(4\sigma_2^2+4\sigma_2+1\right)+(4\sigma_1-2a)(\alpha_r+\alpha_l)} \\ L_{4,3} &= \frac{-(\epsilon(2\sigma_2+1)+(-4\sigma_1+2a)(\alpha_r-\alpha_l))}{\epsilon\left(4\sigma_2^2+4\sigma_2+1\right)+(4\sigma_1-2a)(\alpha_r+\alpha_l)}. \end{aligned}$$

The diagonal elements of $M_\lambda$ are

$$\begin{aligned} \lambda_1 &= 2(2\sigma_1-a) \\ \lambda_2 &= 0 \\ \lambda_3 &= \frac{-\epsilon\left(\epsilon\left(4\sigma_2^2+4\sigma_2+1\right)+(4\sigma_1-2a)(\alpha_r+\alpha_l)\right)}{2(2\sigma_1-a)} \\ \lambda_4 &= \frac{-4\epsilon\left(\alpha_r\epsilon(\sigma_2+1)^2+\alpha_l\epsilon\sigma_2^2+(4\sigma_1-2a)\alpha_l\alpha_r\right)}{\epsilon\left(4\sigma_2^2+4\sigma_2+1\right)+(4\sigma_1-2a)(\alpha_r+\alpha_l)}. \end{aligned}$$

These eigenvalues must be less than or equal to zero to ensure stability of the interface condition. The resulting condition of stability is

$$\sigma_1 \le \frac{a}{2} - \epsilon\left[\frac{\sigma_2^2}{4\alpha_r}+\frac{\sigma_4^2}{4\alpha_L}\right].$$

Combining this expression with the constraints $\sigma_3=\sigma_1-a$ and $\sigma_4=\sigma_2+1$ yields the conditions of Theorem 3.1.

## APPENDIX II: STENCILS

We now present the specific form of the stencils that satisfy the SBP stability requirements and the accuracy requirements shown necessary in the previous numerical study. At second order, the discretization matrix for the advection terms that satisfy the constraint $A_1 = P^{-1}Q$ is

$$A = \frac{1}{2\Delta x}\begin{bmatrix} -2 & 2 & & & & & \\ -1 & 0 & 1 & & & & \\ & \cdot & \cdot & \cdot & & & \\ & & \cdot & \cdot & \cdot & & \\ & & & \cdot & \cdot & \cdot & \\ & & & & -1 & 0 & 1 \\ & & & & & -2 & 2 \end{bmatrix}, \tag{27}$$

where

$$P = \Delta x \begin{bmatrix} \frac{1}{2} & & & & & & \\ & 1 & & & & & \\ & & \cdot & & & & \\ & & & \cdot & & & \\ & & & & 1 & & \\ & & & & & \frac{1}{2} \end{bmatrix}; \quad Q = \frac{1}{2} \begin{bmatrix} -1 & 1 & & & & & \\ -1 & 0 & 1 & & & & \\ & \cdot & \cdot & \cdot & & & \\ & & \cdot & \cdot & \cdot & & \\ & & & \cdot & \cdot & \cdot & \\ & & & & -1 & 0 & 1 \\ & & & & & -1 & 1 \end{bmatrix}. \quad (28)$$

The discretization matrix for the diffusion terms that satisfies the constraint $A_2 = P^{-1}(-S^{\mathrm{T}}R + D)S$ is

$$A = \frac{1}{(\Delta x)^2} \begin{bmatrix} 1 & -2 & 1 & & & & \\ 1 & -2 & 1 & & & & \\ & \cdot & \cdot & \cdot & & & \\ & & \cdot & \cdot & \cdot & & \\ & & & \cdot & \cdot & \cdot & \\ & & & & 1 & -2 & 1 \\ & & & & 1 & -2 & 1 \end{bmatrix}, \quad (29)$$

where

$$S = \frac{1}{\Delta x} \begin{bmatrix} -\frac{3}{2} & 2 & -\frac{1}{2} & & & & \\ & 1 & & & & & \\ & & \cdot & & & & \\ & & & \cdot & & & \\ & & & & \cdot & & \\ & & & & & 1 & \\ & & & & \frac{1}{2} & -2 & \frac{3}{2} \end{bmatrix}; \quad D = \begin{bmatrix} -1 & & & & & & \\ & 0 & & & & & \\ & & \cdot & & & & \\ & & & \cdot & & & \\ & & & & \cdot & & \\ & & & & & 0 & \\ & & & & & & 1 \end{bmatrix} \quad (30)$$

and

$$R = \frac{1}{(\Delta x)} \begin{bmatrix} \frac{4}{9} & -\frac{2}{9} & \frac{2}{9} & & & & & & & & \\ -\frac{2}{9} & \frac{10}{9} & -\frac{10}{9} & & & & & & & & \\ \frac{2}{9} & -\frac{10}{9} & \frac{19}{9} & -1 & & & & & & & \\ & & -1 & 2 & -1 & & & & & & \\ & & & \cdot & \cdot & \cdot & & & & & \\ & & & & \cdot & \cdot & \cdot & & & & \\ & & & & & \cdot & \cdot & \cdot & & & \\ & & & & & & -1 & 2 & -1 & & \\ & & & & & & & -1 & \frac{19}{9} & -\frac{10}{9} & -\frac{2}{9} \\ & & & & & & & & -\frac{10}{9} & -\frac{10}{9} & \frac{2}{9} \\ & & & & & & & & -\frac{2}{9} & -\frac{2}{9} & \frac{4}{9} \end{bmatrix}. \quad (31)$$

The matrix $R$ can be shown to be positive definite (and symmetric).

A fourth-order discretization that satisfies the SBP constraints was originally derived in the work of Strand [12]. The coefficients $r1$ and $r2$ below are different from those proposed by Strand and are chosen so that the resulting discretization $A_1 = P^{-1}Q$ has the standard four-point third-order stencil at the first grid point. This method of constraining free parameters $r1, r2, \ldots$ generalizes to the sixth-order and eighth-order cases, while providing good boundary accuracy and dissipation.

The values of $r1$ and $r2$ are

$$\begin{aligned} r1 &= \frac{-(2177\sqrt{295369} - 1166427)}{25488} \\ r2 &= \frac{(66195\sqrt{53}\sqrt{5573} - 35909375)}{101952} \end{aligned} \tag{32}$$

and the matrices $P$ and $Q$ are

$$P = \Delta x \begin{bmatrix} \frac{-(216r2+2160r1-2125)}{12960} & \frac{(81r2+675r1+415)}{540} & \frac{-(72r2+720r1+445)}{1440} & \frac{-(108r2+756r1+421)}{1296} & \\ \frac{(81r2+675r1+415)}{540} & \frac{-(4104r2+32400r1+11225)}{4320} & \frac{(1836r2+14580r1+7295)}{2160} & \frac{-(216r2+2160r1+665)}{4320} & \\ \frac{-(72r2+720r1+445)}{1440} & \frac{(1836r2+14580r1+7295)}{2160} & \frac{-(4104r2+32400r1+12785)}{4320} & \frac{(81r2+675r1+335)}{540} & \\ \frac{-(108r2+756r1+421)}{1296} & \frac{-(216r2+2160r1+655)}{4320} & \frac{(81r2+675r1+335)}{540} & \frac{-(216r2+2160r1-12085)}{12960} & \\ & & & & 1 \end{bmatrix} \tag{33}$$

and

$$Q = \begin{bmatrix} \frac{(-1)}{2} & \frac{-(864r2+6480r1+305)}{4320} & \frac{(216r2+1620r1+725)}{540} & \frac{-(864r2+6480r1+3335)}{4320} & & & \\ \frac{(864r2+6480r1+305)}{4320} & 0 & \frac{-(864r2+6480r1+2315)}{1440} & \frac{(108r2+810r1+415)}{270} & & & \\ \frac{-(216r2+1620r1+725)}{540} & \frac{(864r2+6480r1+2315)}{1440} & 0 & \frac{-(864r2+6480r1+785)}{4320} & \frac{-1}{12} & & \\ \frac{(864r2+6480r1+3335)}{4320} & \frac{-(108r2+810r1+415)}{270} & \frac{(864r2+6480r1+785)}{4320} & 0 & \frac{8}{12} & \frac{-1}{12} & \\ & & \frac{1}{12} & \frac{-8}{12} & 0 & \frac{8}{12} & \frac{-1}{12} \\ & & & \cdot & \cdot & \cdot & \cdot \end{bmatrix}. \tag{34}$$

Only the inflow boundary portion of the matrices $P$ and $Q$ is shown. The outflow coefficients are the negative transpose of the inflow coefficients. The matrix $P$ is symmetric and positive definite.

The discretization matrix for the diffusion terms that satisfies the constraint $A_2 = P^{-1}(-S^T R + D)S$ is:

$$A = \frac{1}{(\Delta x)^2} \begin{bmatrix} \frac{35}{12} & \frac{-26}{3} & \frac{19}{2} & \frac{-14}{3} & \frac{11}{12} & & & & & \\ \frac{11}{12} & \frac{-5}{3} & \frac{1}{2} & \frac{1}{3} & \frac{-1}{12} & & & & & \\ \frac{-1}{12} & \frac{16}{12} & \frac{-30}{12} & \frac{16}{12} & \frac{-1}{12} & & & & & \\ & \cdot & \cdot & \cdot & \cdot & \cdot & & & & \\ & & \cdot & \cdot & \cdot & \cdot & \cdot & & & \\ & & & \cdot & \cdot & \cdot & \cdot & \cdot & & \\ & & & & \frac{-1}{12} & \frac{16}{12} & \frac{-30}{12} & \frac{16}{12} & \frac{-1}{12} \\ & & & & \frac{-1}{12} & \frac{1}{3} & \frac{1}{2} & \frac{-5}{3} & \frac{11}{12} \\ & & & & \frac{11}{12} & \frac{-14}{3} & \frac{19}{2} & \frac{-26}{3} & \frac{35}{12} \end{bmatrix}, \tag{35}$$

where

$$S = \frac{1}{\Delta x}\begin{bmatrix} -\frac{25}{12} & 4 & -3 & \frac{4}{3} & -\frac{1}{4} & & \\ & 1 & & & & & \\ & & \cdot & & & & \\ & & & \cdot & & & \\ & & & & \cdot & & \\ & & & & & 1 & \\ & & -\frac{1}{2} & -\frac{4}{3} & -3 & -4 & \frac{25}{12} \end{bmatrix}; \quad D = \begin{bmatrix} -1 & & & & & & \\ & 0 & & & & & \\ & & \cdot & & & & \\ & & & \cdot & & & \\ & & & & \cdot & & \\ & & & & & 0 & \\ & & & & & & 1 \end{bmatrix}. \quad (36)$$

The matrix $R$ is too complicated to report here but it can be shown to be positive definite. Note that the matrix $R$ is not needed in the implementation of the scheme and is only used for proving stability. This numerical scheme is referred to as (3,3,3,3-4-3,3,3,3), which denotes the fact that the four points nearest to the boundary are closed with third-order formulas.

A sixth-order discretization that satisfies the SBP constraints was originally derived in the work of Strand [12]. The coefficients $r1, r2$, and $r3$ below are different from those proposed by Strand and are chosen so that the resulting discretization $A_1 = P^{-1}Q$ has the standard six-point fifth-order stencil at the first grid point. This choice produces remarkably good stability characteristics at the boundary. The coefficients are

$$\begin{aligned} r1 &= -3.6224891259957 \\ r2 &= 96.301901955532 \\ r3 &= -609.5813881563. \end{aligned} \quad (37)$$

The symmetric $P$ and nearly skew-symmetric $Q$ matrices have the entries $A_1 = P^{-1}Q$, where

$$\begin{aligned} p(1,1) &= \frac{-(14400\,r2 + 302400\,r1 - 7420003)}{36288000} \\ p(1,2) &= \frac{-(75600\,r3 + 1497600\,r2 + 11944800\,r1 - 59330023)}{21722800} \\ p(1,3) &= \frac{-(9450\,r3 + 202050\,r2 + 1776600\,r1 - 7225847)}{340200} \\ p(1,4) &= \frac{(900\,r2 + 18900\,r1 - 649)}{226800} \\ p(1,5) &= \frac{(86400\,r3 + 1828800\,r2 + 15854400\,r1 - 66150023)}{3110400} \\ p(1,6) &= \frac{(378000\,r3 + 7747200\,r2 + 65167200\,r1 - 279318239)}{188640000} \\ p(2,2) &= \frac{(302400\,r3 + 6091200\,r2 + 49896000\,r1 - 210294289)}{7257600} \\ p(2,3) &= \frac{(3780\,r3 + 82575\,r2 + 741825\,r1 - 2991977)}{34020} \\ p(2,4) &= \frac{(5400\,r3 + 104400\,r2 + 810000\,r1 - 3756643)}{129600} \\ p(2,5) &= \frac{-(529200\,r3 + 11107200\,r2 + 95508000\,r1 - 400851749)}{2419200} \end{aligned}$$

$$
\begin{aligned}
p(2,6) &= \frac{(86400\,r3 + 1828800\,r2 + 15854400\,r1 - 65966279)}{3110400} \\
p(3,3) &= \frac{-(51300\,r3 + 1094400\,r2 + 9585000\,r1 - 39593423)}{64800} \\
p(3,4) &= \frac{(120960\,r3 + 2584800\,r2 + 22680000\,r1 - 93310367)}{181440} \\
p(3,5) &= \frac{(5400\,r3 + 104400\,r2 + 810000\,r1 - 3766003)}{129600} \\
p(3,6) &= \frac{(900\,r2 + 18900\,r1 - 37217)}{226800} \\
p(4,4) &= \frac{-(17100\,r3 + 364800\,r2 + 3195000\,r1 - 13184701)}{21600} \\
p(4,5) &= \frac{(3780\,r3 + 82575\,r2 + 741825\,r1 - 2976857)}{34020} \\
p(4,6) &= \frac{-(1890\,r3 + 40410\,r2 + 355320\,r1 - 1458223)}{68040} \\
p(5,5) &= \frac{(302400\,r3 + 6091200\,r2 + 49896000\,r1 - 213056209)}{7257600} \\
p(5,6) &= \frac{-(75600\,r3 + 1497600\,r2 + 11944800\,r1 - 54185191)}{21722800} \\
p(6,6) &= \frac{-(14400\,r2 + 302400\,r1 - 36797603)}{36288000} \\
q(1,1) &= \frac{(-1)}{2} \\
q(1,2) &= \frac{(415800\,r3 + 8604000\,r2 + 72954000\,r1 - 283104553)}{32659200} \\
q(1,3) &= \frac{(120960\,r3 + 2672640\,r2 + 24192000\,r1 - 100358119)}{6531840} \\
q(1,4) &= \frac{-(25200\,r3 + 542400\,r2 + 4788000\,r1 - 19717139)}{403200} \\
q(1,5) &= \frac{(604800\,r3 + 13363200\,r2 + 120960000\,r1 - 485628701)}{32659200} \\
q(1,6) &= \frac{(41580\,r3 + 860400\,r2 + 7295400\,r1 - 31023481)}{3265920} \\
q(2,2) &= 0 \\
q(2,3) &= \frac{-(9450000\,r3 + 200635200\,r2 + 1747116000\,r1 - 7286801279)}{32659200} \\
q(2,4) &= \frac{(21168000\,r3 + 449049600\,r2 + 3907008000\,r1 - 16231108387)}{32659200} \\
q(2,5) &= \frac{-(165375\,r3 + 3516300\,r2 + 30665250\,r1 - 126996371)}{453600}
\end{aligned}
\tag{38}
$$

$$q(2,6) = \frac{(604800\,r3 + 13363200\,r2 + 120960000\,r1 - 482536157)}{32659200}$$

$$q(3,3) = 0$$

$$q(3,4) = \frac{-(6993000\,r3 + 148096800\,r2 + 1286334000\,r1 - 5353075351)}{8164800}$$

$$q(3,5) = \frac{(21168000\,r3 + 449049600\,r2 + 3907008000\,r1 - 16212561187)}{32659200}$$

$$q(3,6) = \frac{-(75600\,r3 + 1627200\,r2 + 14364000\,r1 - 58713721)}{1209600}$$

$$q(4,4) = 0$$

$$q(4,5) = \frac{-(9450000\,r3 + 200635200\,r2 + 1747116000\,r1 - 7263657599)}{32659200}$$

$$q(4,6) = \frac{(604800\,r3 + 13363200\,r2 + 120960000\,r1 - 485920643)}{32659200}$$

$$q(5,5) = 0$$

$$q(5,6) = \frac{(415800\,r3 + 8604000\,r2 + 72954000\,r1 - 286439017)}{32659200}$$

$$q(6,6) = 0.$$

The matrix $P$ is symmetric and positive definite for this choice of parameters.

The discretization matrix for the diffusion terms that satisfies the constraint $A_2 = P^{-1}(-S^T R + D)S$ is

$$A = \frac{1}{180(\Delta x)^2}\begin{bmatrix} +812 & -3132 & +5265 & -5080 & +2970 & -972 & +137 \\ +137 & -147 & -255 & +470 & -285 & +93 & -13 \\ -13 & +228 & -420 & +200 & +15 & -12 & +2 \\ 2 & -27 & 270 & -490 & 270 & -27 & 2 \end{bmatrix}, \qquad (39)$$

where

$$S = \frac{1}{\Delta x}\begin{bmatrix} \frac{(-49)}{20} & 6 & \frac{(-15)}{2} & \frac{20}{3} & \frac{(-15)}{4} & \frac{6}{5} & \frac{(-1)}{6} \\ & 1 & & & & & \\ & & . & & & & \end{bmatrix}, \quad D = \begin{bmatrix} -1 & & \\ & 0 & \\ & & . \end{bmatrix}. \qquad (40)$$

The matrix $R$ is too complicated to report here but can be shown to be positive definite. Again, the matrix $R$ is not necessary for implementing the numerical method, being used only for proving stability.

Finally, we note that SBP boundary closures are more complicated than conventional discretizations and that inadvertent mistakes in their implementation could have profound consequences on the stability and accuracy of the procedure. As such, we provide "black-box" subroutines which implement all the derivative operators used in this study. Send requests for these routines to m.h.carpenter@larc.nasa.gov.

## REFERENCES


1. D. A. Kopriva, Multidomain spectral solution of the Euler gas-dynamics equations, *J. Comput. Phys.* **96**, 428 (1991).
2. D. A. Kopriva, Multidomain spectral solution of compressible viscous flows, *J. Comput. Phys.* **115**, 184 (1994).
3. D. A. Kopriva and J. H. Kolias, A conservative staggered-grid Chebyshev multidomain method for compressible flows, *J. Comput. Phys.* **125**, 244 (1996).
4. J. S. Hesthaven and D. Gottlieb, A stable penalty method for the compressible Navier–Stokes equations. I. Open boundary conditions, *SIAM J. Sci. Comput.* **17**(3), 579 (1996).
5. J. S. Hesthaven, A stable penalty method for the compressible Navier–Stokes equations. II. One-dimensional domain decomposition schemes, *SIAM J. Sci. Comput.* **18**(3), 658 (1997).
6. J. S. Hesthaven, A stable penalty method for the compressible Navier–Stokes equations. III. Multidimensional domain decomposition schemes, *SIAM J. Sci. Comput.*, in press.
7. H.-O. Kreiss and G. Scherer, Finite element and finite difference methods for hyperbolic partial differential equations, in *Mathematical Aspects of Finite Elements in Partial Differential Equations* (Academic Press, New York, 1974).
8. P. Olsson, High-order difference methods and data-parallel implementation, Ph.D. thesis, Uppsala University, Department of Scientific Computing, 1992.
9. P. Olsson, Summation by parts, projections, and stability I, *Math. Comp.* **64**, 1035 (1995).
10. P. Olsson, Summation by parts, projections, and stability II, *Math. Comp.* **64**, 1473 (1995).
11. B. Strand, High-order difference approximations for hyperbolic initial boundary value problems, Ph.D. thesis, Department of Scientific Computing, Uppsala University, 1996.
12. B. Strand, Summation by parts for finite difference approximations for $d/dx$, *J. Comput. Phys.* **110**(1), 47 (1994).
13. M. H. Carpenter, D. Gottlieb, and S. Abarbanel, Time-stable boundary conditions for finite-difference schemes solving hyperbolic systems: Methodology and application to high-order compact schemes, *J. Comput. Phys.* **111**, 2 (1994).
14. M. H. Carpenter and D. Gottlieb, Spectral methods on arbitrary grids, *J. Comput. Phys.* **129**, 74 (1996).
15. M. H. Carpenter and J. Otto, High-order cyclo-difference techniques: An alternative to finite differences, *J. Comput. Phys.* **118**, 242 (1995).
16. P. D. Lax and B. Wendroff, Systems of conservation laws, *Comm. Pure Appl. Math.* **13**, 217 (1960).
17. B. Gustafsson, The convergence rate for difference approximations to mixed initial boundary value problems, *Math. Comp.* **29**(130), 396 (1975).